

# Effect of a partial coverage of quasar broad-line regions by intervening H<sub>2</sub>-bearing clouds

D. D. Ofengeim<sup>1,2</sup> • S. A. Balashev<sup>2,3</sup> •  
A. V. Ivanchik<sup>2,3</sup> • A. D. Kaminker<sup>2,3</sup> •  
V. V. Klimenko<sup>2,3</sup>

## Abstract

We consider the effect of a partial coverage of quasar broad-line regions (QSO BLRs) by intervening H<sub>2</sub>-bearing clouds when a part of quasar (QSO) radiation passes by a cloud not taking part in formation of an absorption-line system in the QSO spectrum. That leads to modification of observable absorption line profiles and consequently to a bias in physical parameters derived from standard absorption line analysis. In application to the H<sub>2</sub> absorption systems the effect has been revealed in the analysis of H<sub>2</sub> absorption system in the spectrum of Q 1232+082 (see Ivanchik et al. 2010, Balashev et al. 2011). We estimate a probability of the effect to be detected in QSO spectra. To do this we derive distribution of BLR sizes of high-*z* QSOs from Sloan Digital Sky Survey (SDSS) Data Release 9 (DR9) catalogue and assume different distributions of cloud sizes. We conclude that the low limit of the probability is about 11%. The latest researches shows that about a fifth of observed H<sub>2</sub> absorption systems can be partially covered. Accounting of the effect may allow to revise significantly physical parameters of interstellar clouds obtained by the spectral analysis.

**Keywords** quasars: absorption line systems – clouds; cosmology – observations: ISM

## 1 Introduction

An effect of the partial coverage occurs when an absorbing cloud does not fully cover an emission source. It is mostly probable at a situation in which an angular size of the source is comparable with a size of the absorbing object. The partial coverage is greatly important for spectroscopic studies including a choice of an appropriate model of the absorption-line systems (ALSs), which is necessary to derive physical parameters of an absorbing cloud from spectral analysis. In the simplest case of partial coverage the part of radiation from the emission source passes by the absorbing cloud. It results in an additional residual flux at the bottom of absorption lines registered in the spectrum with respect to the zero-flux level. This effect is more pronounced in the case of highly saturated lines.

It should be emphasized that the most typical situation for investigations of interstellar medium is when angular size of an absorbing cloud is much larger than an angular size of a background source which can be considered as a point-like object. In such cases the effects of the partial coverage are very unlikely and the observer uses simple absorption-line profiles defined by the optical depth  $\tau(\lambda)$  according to the Bouguer-Lambert-Beer law. However, this approach ceases to be universal for studies of the ALSs in QSO spectra, especially for relatively compact H<sub>2</sub> clouds whose sizes can be comparable with sizes of QSO emission regions.

QSOs are the powerful active galactic nuclei located at cosmological distances (up to  $z \sim 7$ ). Their high luminosity allows to detect their spectra and to study medium between QSOs and the observer via analysis of the ALSs imprinted in their spectra. Remind that the ALSs detected in QSO spectra can be classified in two general categories: *intrinsic* and *intervening*. *Intrinsic* absorption systems are related to a region in the close vicinity of the central QSO machine or the host

---

D. D. Ofengeim

S. A. Balashev

A. V. Ivanchik

A. D. Kaminker

V. V. Klimenko

<sup>1</sup>St.-Petersburg Academic University, 8/3 Khlopina street, 194021 St.-Petersburg, Russia

<sup>2</sup>Ioffe Physical-Technical Institute, Politekhnikeskaya 26, 194021 St.-Petersburg, Russia

<sup>3</sup>St.-Petersburg State Polytechnical University, Politekhnikeskaya 29, 195251 St.-Petersburg, Russia

galaxy. *Intervening* absorption systems appear from intergalactic medium and interstellar medium of galaxies remote from the QSO. It was found that the effects of partial coverage, breaking the universal conception of a point-like source against an extended absorber, is a rather frequent phenomenon for the intrinsic ALSs in QSO spectra (Petitjean et al. 1994).

However, up to recently in the case of intervening ALSs the effects of partial coverage were believed to be unlikely. Actually, the projected sizes of typical intervening absorbers are much larger than quasar emission regions. The emission regions of QSOs in UV and optical range have been constrained by a size of  $\lesssim 1$  pc. For example, reverberation mapping establishes the relationship between the BLR size and the luminosity and yields a BLR size of  $R_{\text{BLR}} \sim 0.2$  pc (Kaspi et al. 2007; Chelouche and Daniel 2012) for high redshift luminous quasars. Differential microlensing allows one to estimate the size of the BLR  $\sim 0.1$  pc (Sluse et al. 2011). The observations of gamma-ray emission constrain the size of the jet extension to a few parsecs (Abdo et al. 2010). On the other hand, majority of ALSs constitute the Ly- $\alpha$  forest, which are related to intergalactic clouds with sizes well exceeding 10 kpc (Rauch 1998). Sizes of diffuse atomic clouds inside intervening galaxies are considered to imprint the damped Ly- $\alpha$  systems (DLAs), or sub-DLAs, can be roughly estimated as 10 pc – 1 kpc. At last, the Lyman-limit systems (LLS), as well as Mg II and C IV absorbers, seems to correspond also to kpc-scale clouds in the halo of the intervening galaxies.

Nevertheless, the partial coverage of Mg II system in the spectrum of the QSO, APM 08279+5255, was firstly reported by Ledoux et al. (1998). However, it had been found some later that this was very peculiar case of the partial coverage due to a gravitational lensing of the background QSO (see Ledoux et al. 1998; Ibata et al. 1999). More definitely the effect of partial coverage has been revealed in the case of H I 21cm absorption lines measurements in the DLA system (Kanekar et al. 2009). Actually, the emission regions of radio-loud QSOs at a wavelength 21 cm can well exceed a size of 10 kpc and typically consist of compact few pc cores and extended dilute envelopes. The effect of partial coverage essentially alters derived spin temperature  $T_s$  of the neutral gas absorber (Kanekar et al. 2009).

Molecular bearing ALSs are another type of currently observed absorption systems in QSO spectra which may have projected sizes comparable with a size of QSO emission region. These systems include molecular absorption lines (predominantly H<sub>2</sub>, in some cases – HD and CO) and refer to the diffuse and translucent molecular phases of the interstellar medium

(Snow and McCall 2006). Estimated number density of this system is  $\gtrsim 10 \text{ cm}^{-3}$  at the column density  $\lesssim 10^{20} \text{ cm}^{-2}$ , consequently these clouds constrained by pc or even sub-pc sizes (see Sect.3.1).

The major part of QSO radiation is generated by an accretion disk (AD) around the black hole and forms a continuous spectrum. Characteristic size of the AD is considered to be  $\lesssim 3 \times 10^{-3}$  pc (e.g. Blackburne et al. 2011; Jiménez-Vicente et al. 2012). Thus this source may be treated as a point-like object fully covered by molecular clouds. On the other hand, there is still an extended region around the AD of relatively dense and warm partly ionized gas, called a broad-line region (BLR), where broad emission lines are formed, that leads to some additional enhancement of the continuum in QSO spectra. The angular size of this region at least an order of magnitude exceeds the typical angular sizes of ADs and may be comparable with sizes of H<sub>2</sub> molecular clouds. Therefore an incomplete coverage of BLRs by molecular clouds situated on the line-of-sight between the QSO and observer becomes quite probable.

The partial coverage of a BLR by the intervening H<sub>2</sub> absorption cloud was reported by Ivanchik et al. (2010) and investigated in details by Balashev et al. (2011). It was demonstrated that the H<sub>2</sub>-bearing cloud ( $z_{\text{abs}} = 2.34$ ) covers completely the QSO 1232+082 ( $z_{\text{em}} = 2.57$ ) intrinsic continuum source, but only a part of the BLR.

There are also other possibilities for the partial coverage effect: (i) jet emission can be scattered/re-emitted by medium in the quasar host galaxy, which is remote from the AD and BLR. In this case the observer detects the partial coverage of a continuous spectrum. This is the most probable explanation of the recently revealed partial coverage of the Q 0528-250 continuous spectrum by H<sub>2</sub> absorption system at  $z=2.811$  (Klimenko et al. 2015). (ii) The calculation of galaxies evolution shows that a galaxy at high redshifts can have several supermassive black holes (SMBHs; binary, triple or quadruple systems of SMBHs, e.g. Kulkarni and Loeb 2012), in particular, one of SMBHs can remain unscreened by an absorbing molecular cloud. (iii) The observer can register UV emission of a QSO host galaxy much more extended than a BLR. (iv) The partial coverage can be caused by gravitational lensing (e.g. the case of APM08279+5255) of a galaxy or a galaxy cluster located between a quasar and intervening clouds.

The effect of partial coverage leads to serious changes of parameters derived from an analysis of QSO spectra (e.g. column densities of absorbers, Ivanchik et al. 2010; Balashev et al. 2011; Klimenko et al. 2015). So it is worthwhile to estimate a probability to find the par-

tial coverage of a QSO BLR by an intervening  $H_2$  absorption system. Other appearances of the partial coverage (listed above), apparently, lead only to increase the probability.

Following Balashev et al. (2011), one can introduce a *flux coverage factor*  $f$  as the ratio of a light flux comprising the absorption systems imprinted in its spectrum to the total flux from a quasar. In the present paper we calculate a probability to reveal the partial coverage of a QSO BLR located at some redshift  $z_q$  by  $H_2$  ALS at redshift  $z_c$  (cloud) with coverage factor  $f < f_0$  ( $f_0$  is a fixed value, see below). We consider an arbitrary angular distance between line-of-sights to the centres of the cloud and BLR, as well as an arbitrary ratio  $\kappa$  of the cloud to BLR transverse sizes.

The paper significantly develops our previous work (Ofengeim et al. 2013) and is organized as following. At first, we proceed from an oversimplified assumption of uniformity of the radiation flux from the whole BLR region ignoring the luminous point-like AD in the centre of the QSO. In Section 2 we introduce a geometrical coverage factor  $g \equiv f$  and consider the main parameters controlling  $g$ . In Section 3.1 we calculate a probability to reveal factor  $g < g_0$ , where  $g_0$  is also a fixed value (an analogue of  $f_0$ ), for certain distributions of the main parameters. In Section 3.2 we discuss similar probability but for more realistic coverage factor  $f$  determined as the ratio of radiation fluxes, taking into account nonuniformity of the radiation flux and including the intense AD radiation. Sections 3.3 and 4 present a special consideration of the dependence of the factor  $f$  on the redshifts  $z_q$  and  $z_c$ . In Section 5 we discuss obtained results and their relation to observations.

## 2 Geometry of partial coverage

In this work we use a toy model to describe the emission regions of QSOs and absorbing clouds. The geometry of this model is presented in Fig. 1,2. The transverse sizes of the BLR and the cloud are designated as  $l_q$  and  $l_c$ , the angular size of the BLR is designated by  $\theta_q$  (hereinafter angles are in radians), a corresponding angle for the cloud can be denoted as  $\theta_c$  (is not shown in Fig. 1). The light from the BLR propagates through the Universe and it is registered by the observer. The observer detects an emission within a light cone restricted by an angle  $\theta_q$  or a solid angle  $\Omega_q$  comprising the whole flux from the BLR. Some part of light from the BLR is partly shielded by the cloud in such a way that molecules inside the cloud imprint a set of absorption lines (or ALS) in the initial spectrum. This part is bounded by a solid angle (of coverage)  $\Omega_{cov}$ .

The rest light can pass by the cloud and come to the observer without formation of ALSs in its spectrum. This flux of radiation may be approximately estimated as a flux comprised by a solid angle  $\Omega_{uncov} = \Omega_q - \Omega_{cov}$ . In result the observer detects a complex radiation from the QSO with spectrum integrated over angles.

Let us determine a *geometrical* coverage factor  $g$  as a simplest way to estimate factor  $f$ . If we assume that fluxes from covered and uncovered parts of the BLR are uniformly distributed within their solid angles, then factor  $g$  may be estimated as a ratio of the solid angle  $\Omega_{cov}$  to the whole solid angle  $\Omega_q$ :

$$g = \frac{\Omega_{cov}}{\Omega_q}, \quad (1)$$

where at  $\theta_q \ll 1$  we can write  $\Omega_q = \pi\theta_q^2$ . We imply that  $g \equiv f$  in the case of pure geometrical estimations. Actually, the factor  $g$  may essentially differ from  $f$  because it does not take into account nonuniformity of fluxes within the solid angles (see Section 3.2).

Thereafter it is convenient to express all angular values in units of  $\theta_q$  and all solid angles – in units of  $\Omega_q$ . Thus a relative angle between directions to the centres of QSO and cloud (angular deviation) is determined as

$$\delta = \frac{\Delta\theta}{\theta_q}, \quad (2)$$

and the relative angle size of a cloud becomes

$$\rho = \frac{\theta_c}{\theta_q}. \quad (3)$$

An angle size  $\theta$  of an object with a transverse size  $l$  at the cosmological redshift  $z$  may be determined by a standard way (e.g. Zeldovich and Novikov; Kayser et al. 1997) as

$$\theta = \frac{l}{2 D_A(z)}, \quad (4)$$

where  $D_A(z)$  is an angular diameter distance. In the standard  $\Lambda$ CDM cosmological model the value  $D_A(z)$  to a cosmologically distant object at the redshift  $z$  is (e.g. Zeldovich and Novikov; Kayser et al. 1997)

$$D_A(z) = \frac{c}{H_0} \frac{1}{1+z} \int_0^z \frac{dz'}{\sqrt{\Omega_m(1+z')^3 + \Omega_\Lambda}}, \quad (5)$$

where  $c$  is the speed of light,  $H_0 = 100 h \text{ km s}^{-1}$  is the present Hubble constant,  $c/H_0 \approx 2.998 h^{-1} \text{ Gpc}$ ;  $\Omega_m$  is the dimensionless matter density parameter and  $\Omega_\Lambda = \Lambda c^2/(8\pi G)$  is determined by the cosmological constant  $\Lambda$ ,  $G$  is the gravitational constant; hereafter we assume that  $\Omega_m = 0.3$  and  $\Omega_\Lambda = 0.7$  (Planck Collaboration et al. 2014)

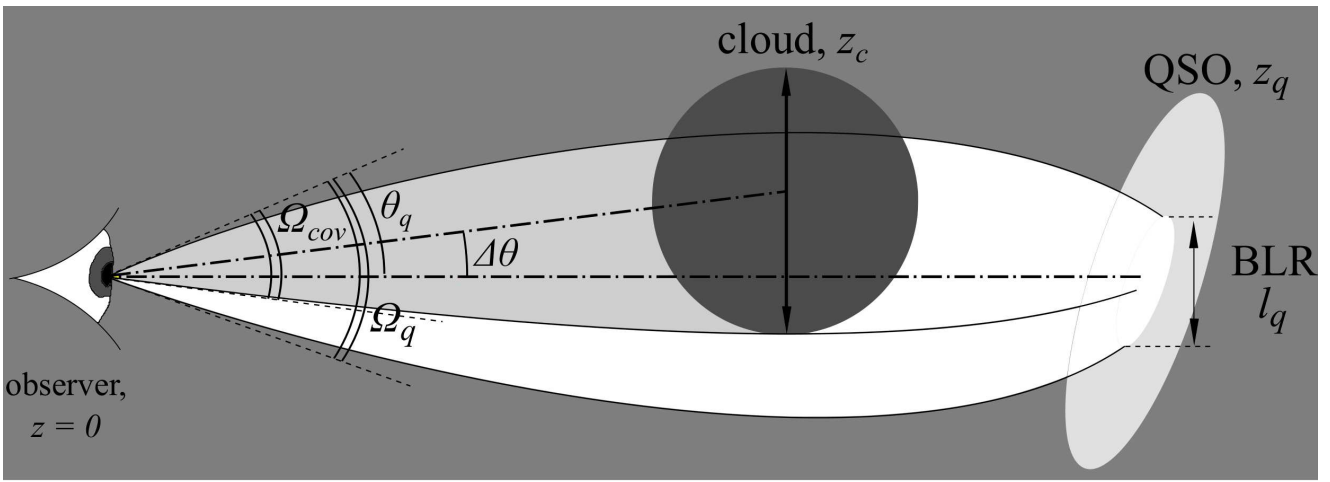


**Fig. 1** Schematic illustration of an absorption cloud at a transverse size  $l_c$  (dark grey circle) situated between the observer and QSO BLR with a transverse size  $l_q$  (white ellipse in the centre of QSO); the wider ellipse around BLR (light grey) symbolizes a QSO host galaxy;  $\theta_q$  is an angular size of BLR,  $\Delta\theta$  is an angle between two line-of-sights from the observer to the centres of QSO and cloud;  $z_q$  and  $z_c$  are redshifts of the QSO and cloud;  $\Omega_q$  is a solid angle (light cone) of the whole BLR radiation flux,  $\Omega_{cov}$  is a solid angle of a part of BLR flux passed through the cloud. Radiation from the QSO without traces of  $H_2$ -absorption systems in its spectrum is shown as a white area of the light cone and radiation containing the absorption systems – as a light grey area. In general case the light cone is curved due to the expansion of the Universe.

Using Eq. (4) one can rewrite Eq. (3) as

$$\rho(\kappa, z_q, z_c) = \kappa \frac{D_A(z_q)}{D_A(z_c)}, \quad (6)$$

where the relative angular size of the cloud is expressed through the ratio of transverse sizes of the cloud and QSO

$$\kappa = \frac{l_c}{l_q}. \quad (7)$$

The coverage factor  $g$  is a function of  $\rho = \rho(\kappa; z_q, z_c)$  and  $\delta$ . Fig. 2 demonstrates four basic types of relative positions of two circles conventionally referred to the BLR and cloud projected on the sky.

These types corresponding to special dependence  $g = g(\rho, \delta)$  can be formalized as follows:

(i) *Full coverage*:  $1 + \delta \leq \rho$ . All flux from the QSO BLR goes through the cloud,  $g = 1$ . Up to recently, only this case has been considered in literature in application to intervening  $H_2$  clouds.

(ii) *Partial ring-shaped coverage*:  $\rho + \delta \leq 1$ . The angular size of the BLR exceeds the angular size of the cloud plus the angular deviation. In this case  $g = \rho^2$ .

(iii) *Crescent-like coverage*:  $|\rho - 1| < \delta < \rho + 1$ . After some calculations one can obtain

$$g(\rho, \delta) \equiv s(\rho, \delta) = \frac{\rho^2}{\pi} \arccos \frac{\rho^2 + \delta^2 - 1}{2\rho\delta} + \frac{1}{\pi} \arccos \frac{1 + \delta^2 - \rho^2}{2\delta} - \frac{1}{2\pi} \sqrt{[\rho^2 - (\delta - 1)^2][(\delta + 1)^2 - \rho^2]}. \quad (8)$$

(iv) *Full noncoverage*:  $1 + \rho \leq \delta$ . Relative angular distance is large and the cloud remains unobservable in the QSO spectrum. In this case  $g = 0$ .

One can summarize all cases (i)–(iv):

$$g(\kappa, \delta; z_q, z_c) = \begin{cases} 1; & \text{(i)} \\ \rho^2(\kappa; z_q, z_c); & \text{(ii)} \\ s[\rho(\kappa; z_q, z_c), \delta]; & \text{(iii)} \\ 0; & \text{(iv)} \end{cases} \quad (9)$$

### 3 Distribution of coverage factor

#### 3.1 Geometrical coverage factor

Let us calculate the cumulative distribution function (CDF)  $P(g < g_0)$ , which describes the probability to detect an absorption system in QSO spectrum with geometrical coverage factor  $g$  not exceeding a value  $g_0$ . Since one can reveal the cloud only detecting absorption lines in QSO spectra, the case of full noncoverage  $g = 0$  is equivalent to the absence of an observed cloud.

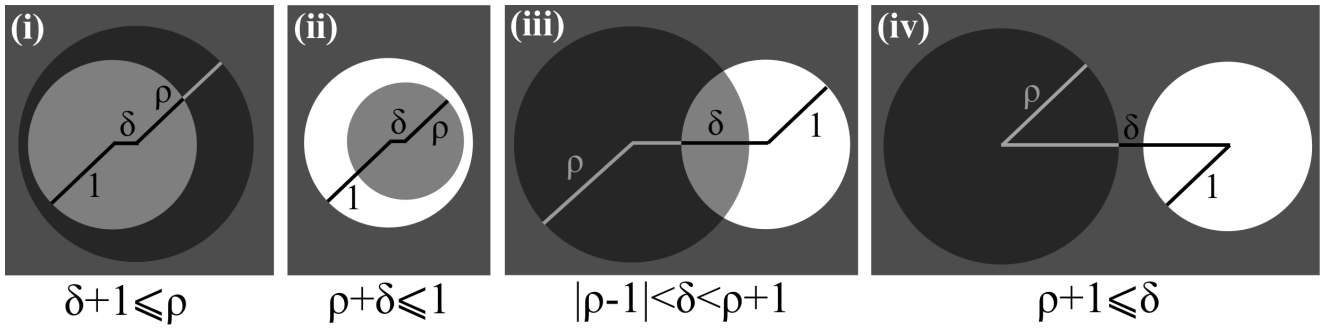


**Fig. 2** Four types of coverage (grey regions) of QSO BLRs (white circles) by clouds (black circles) in the observer reference frame: (i) full coverage,  $g = 1$  (widely accepted case, white circle coincides with grey one); (ii) partial *ring-shaped* coverage,  $0 < g < 1$  (black circle coincides with grey one); (iii) *crescent-like* coverage,  $0 < g < 1$ ; (iv) full *noncoverage*,  $g = 0$ . All angular sizes are represented in units of  $\theta_q$ : the angular size (radius) of the BLR is 1, the radius of the cloud is  $\rho$ , and the angular deviation is  $\delta$  (see text).

Therefore we can put (rather conventionally) that the probability of full noncoverage is  $P(g = 0) = 0$ .

More specifically, to detect an absorption system in a spectrum it is necessary that a cloud totally cover the QSO AD<sup>1</sup>. In contrast, if the cloud partially cover only BLR and does not cover AD, H<sub>2</sub> molecular absorption lines associated with the cloud in the spectrum will be detectable only in surroundings of the top of quasar emission lines blueshifted of Ly $\alpha$  (e.g. C III or Ly $\beta$ +O VI, see Fig. 7). However, in such a case the effect of the partial covering would be difficult to identify, since only several weak absorption lines of the H<sub>2</sub> ALS could be expected. These lines would be hardly detectable against the numerous Ly-alpha forest lines in the spectrum. It gives an additional restriction on the angular deviation:  $\delta < \rho$ , or  $P(\delta > \rho) = 0$ .

Let us add, that the effect of the partial coverage can be observed also for C IV emission line (redshifted of Ly $\alpha$ ) using C I (neutral carbon) absorption lines associated with H<sub>2</sub> (Ivanchik et al. 2010; Balashev et al. 2011), but this case is not considered in this paper.

The CDF  $P(g < g_0)$  can be determined through the distributions of two random values  $\kappa'$  and  $\delta'$ . Let us determine the probability density functions (PDFs) for these two distributions:  $p_\kappa(\kappa)$  and  $p_\delta(\delta|\kappa)$ , respectively, the latter value being the conditional PDF of the occurrence of  $\delta' = \delta$  at a given value  $\kappa' = \kappa$ . Following to the standard definitions of the Probability theory one can introduce the relations between these PDFs and differential probabilities:  $P(\kappa < \kappa' < \kappa + d\kappa) = p_\kappa(\kappa) d\kappa$  and  $P(\delta < \delta' < \delta + d\delta) = p_\delta(\delta|\kappa) d\delta$ , and as a consequence

to write

$$P(g < g_0) = \int_0^\infty \int_0^\infty p_\delta(\delta|\kappa) p_\kappa(\kappa) \Theta[g_0 - g(\kappa, \delta)] d\delta d\kappa. \quad (10)$$

where  $\Theta(x)$  is the Heaviside function. One can optimize calculations using the reciprocal relation  $\kappa(g, \delta)$  given in Eqs. (26) and (27) of Appendix. Then integration over  $\kappa$  in Eq. (10) should goes from 0 to  $\kappa(g_0, \delta)$ .

For simplicity, we assume the uniform mutual distribution of QSO and cloud centres on the sky and get  $p_\delta(\delta) \propto \delta$ . To obtain a normalization function for  $p_\delta(\delta)$  we use the condition  $\delta < \rho$  of the reliable detection of H<sub>2</sub> ALS (see above). In result we obtain

$$p_\delta(\delta|\kappa) = \frac{2\delta}{[\rho(\kappa)]^2} \Theta[\rho(\kappa) - \delta]. \quad (11)$$

It was chosen that  $z_q = 2.57$ ,  $z_c = 2.33$  in all calculations employing Eq. (6) for  $\rho(\kappa, z_q, z_c)$ , i.e. they refer to the case of the partial coverage of Q 1232+082 (Balashev et al. 2011). The dependence of results on the redshifts will be investigated in Section 3.3.

The PDF  $p_\kappa$  with respect to  $\kappa$  may be represented as

$$p_\kappa(\kappa) = 2 \int_0^\infty p_{cloud}(2\kappa r) p_{qso}(r) r dr, \quad (12)$$

where  $p_{cloud}$  and  $p_{qso}$  are PDFs for linear sizes of clouds  $l_c = 2\kappa r$  and radii  $r = l_q/2$  of BLRs, respectively; in derivation of Eq. (12) it is used that  $dl_c = 2r d\kappa$ ; factors  $d\kappa$  are reduced in both sides of Eq. (12).

To obtain  $p_{qso}(r)$  we exploit an empirical equation by Kaspi et al. (2005) between the radius  $r$  and QSO luminosity

$$\frac{r}{10 \text{ light-days}} = AL^B, \quad (13)$$

<sup>1</sup>Remind that the AD generates the most part of continuum radiation

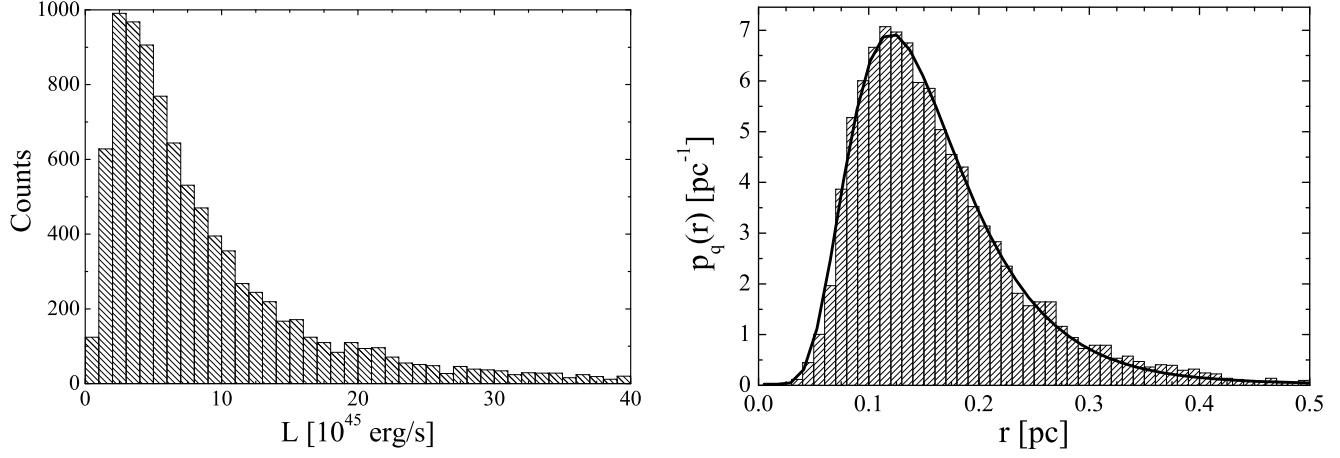


**Fig. 3** *Left panel:* Histogram (hatched bars) of QSO-luminosities sampled at a wavelength of  $1450 \text{ \AA}$  from the data of SDSS DR9, QSOs are chosen under condition of the presence of DLAs in their spectra; *right panel:* probability density function (PDF) of BLR radii, hatched histogram bars form a distribution obtained with using Eq. (13) and the data shown in the left panel; solid line is the resulting lognormal approximation.

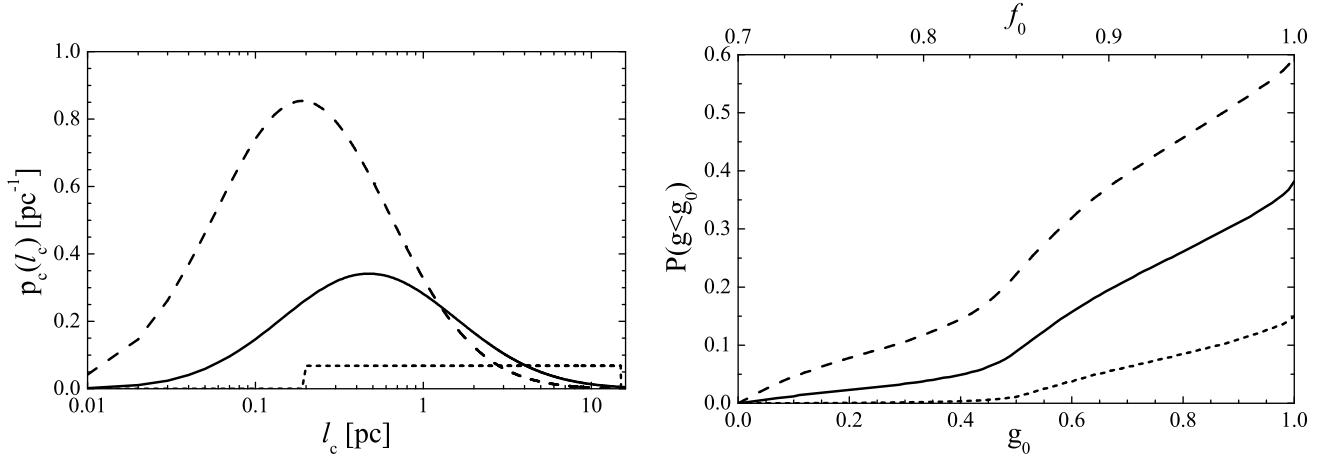


**Fig. 4** *Left panel:* Three types of cloud sizes,  $l_c$ , distribution. Short-dashed curve is the uniform distribution within an interval of  $0.2 \leq l_c \leq 15$  pc, solid curve is the lognormal distribution on a condition that the values  $l_c$  with 90% probability belong to the same interval  $0.2 \leq l_c \leq 15$  pc, long-dashed curve is the lognormal distribution on a condition that the most probable value is  $l_c = 0.2$  pc (see text). *Right panel:* the cumulative distribution function  $P(g < g_0)$  — the probability to detect absorption systems in a QSO spectrum (represented at  $z_q = 2.57$  and  $z_c = 2.33$ ) with the geometrical coverage factor  $g < g_0$ . The upper argument,  $f_0$  (flux coverage factor), determined by a scaling  $f_0 = 0.3g_0 + 0.7$  in such a way that the cumulative distribution functions  $P(f < f_0)$  remains unalterable. Types of lines are the same as in the *left panel*.

where  $L = \lambda L_\lambda / (10^{44} \text{ [erg/s]})$  is the normalized QSO luminosity at a fixed QSO-restframe wavelength  $\lambda$ ,  $A$  and  $B$  - numerical coefficients. To estimate QSO luminosity distribution we used QSO spectra from SDSS DR 9, (see Ahn and et al. 2012). It is commonly accepted that due to high column density  $\text{H}_2$ -cloud associated with large amount of neutral hydrogen, i.e. associated with DLAs. We used the sample of DLAs bearing QSOs (Noterdaeme and et al. 2012) from the whole SDSS DR9 QSOs sample. Choosing in Eq. (13) luminosities at the QSO-restframe wavelength  $\lambda = 1450 \text{ \AA}$  and quantities  $A = 2.12$ ,  $B = 0.496$  (errors omitted) we can calculate a required distribution  $p_{qso}(r)$ .

Actually, Fig. 3 shows the distributions of QSO (DLA) luminosities at  $\lambda = 1450 \text{ \AA}$  (left panel) and  $p_{qso}(r)$  calculated for BLR radii (right panel). One can see that the lognormal approximation

$$p_{qso}(r) = \frac{1}{\sqrt{2\pi}w} \frac{e^{-\frac{(\ln \frac{r}{r_0})^2}{2w^2}}}{r}, \quad (14)$$

where  $w = 0.426 \pm 0.003$  and  $r_0 = (0.1442 \pm 0.0004) \text{ pc}$  obtained by the least square method, proves to be good.

The situation with a distribution  $p_{cloud}(l_c)$  for  $\text{H}_2$  molecular clouds is still more uncertain. Absorption systems of  $\text{H}_2$  detected at high redshifts are referred to the cold neutral medium, which has a lower limit of the number density about  $1 \div 10 \text{ cm}^{-3}$  (e.g. see Liszt 2002). It gives  $l_c < 3 \div 30 \text{ pc}$  for typical measurable column densities  $\sim 10^{19} \div 10^{20} \text{ cm}^{-2}$ . On the other hand, the analysis of  $\text{H}_2$  absorption system in the spectrum of Q1232+082 (Balashev et al. 2011) yields  $l_c \sim 0.2 \text{ pc}$ . Therefore we employ for our estimation two modeled distributions: (1) the uniform distribution within an interval  $[0.2, 15.0] \text{ pc}$

$$p_{cloud}^{(1)}(l_c) = \frac{1}{b-a} \Theta(l_c - a) \Theta(b - l_c), \quad (15)$$

where  $a = 0.2 \text{ pc}$  and  $b = 15.0 \text{ pc}$ . One can expect that this model gives overestimated sizes of the clouds and consequently underestimated values of  $P(g > g_0)$ . (2) The lognormal distribution

$$p_{cloud}^{(2)}(l_c) = \frac{1}{\sqrt{2\pi}u} \frac{e^{-\frac{(\ln \frac{l_c}{l_0})^2}{2u^2}}}{l_c}, \quad (16)$$

where parameters  $u$  and  $l_0$  are choosing also for two cases. The first one is  $u = 1.2$  and  $l_0 = 0.8 \text{ pc}$ , it corresponds to the fixed maximum of the distribution Eq. (16) or to the most probable size at  $l_c = 0.2$ . The second one satisfies to the condition that 90% clouds fall into the interval  $[0.2, 15.0] \text{ pc}$ . In that case  $u = 1.3$  and  $l_0 = 2.0 \text{ pc}$ .

The left panel in Fig. 4 demonstrates three types of the PDF for the cloud sizes  $l_c$  defined by Eqs. (15) and (16) with two sets of parameters  $u$  and  $l_0$ . The right panel shows the integral probability  $P(g < g_0)$  as functions of  $g_0$  calculated with the use of Eqs. (10), (11), and (12) at all three types of distribution  $p_{cloud}(l_c = 2\kappa r)$  discussed above. Let us emphasize the strong dependence of the probability distribution on the distribution of cloud sizes. Nevertheless, even the most conservative estimation of the probability to reveal  $g < 0.98$  proves to be  $\approx 15\%$ , where  $g_0 = 0.98$  corresponds to the minimal measurable noncoverage factor:  $1 - g_0 \geq 0.02$  (Klimenko et al. 2015).

### 3.2 Flux coverage factor

In contrast with the oversimplified geometrical coverage factor  $g$  one can introduce the factor  $f$  as a ratio of radiation fluxes, which is more relevant to a spectral analyses:

$$f = \frac{I_{cov}}{I_{qso}}, \quad (17)$$

where  $I_{cov}$  is the flux of the quasar radiation passed through the cloud,  $I_{qso}$  is the total flux. This value may be called as a *flux coverage factor*. In the case of uniform distribution of the flux over a solid angle  $\Omega_q$  we have  $I_{cov} \propto \Omega_{cov}$ ,  $I_{qso} \propto \Omega_q$  and the flux factor  $f$  would be equal to  $g$ .

Let us regard, some arbitrary, that the flux from the AD characterized by a continuum spectrum constitutes about 70% of the whole intensity. The rest 30% of the flux originates from the BLR (Fig. 5) and represents a set of broad emission lines which also raises a level of continuum in some parts of the spectrum<sup>2</sup>.

If the AD is covered totally but the BLR is covered partially (*left panel* in Fig. 5), the partial coverage effect ( $f < 1$ ) will be detected only in those absorption lines which are located around the top of QSO emission lines. Outside the wide emission lines the partial coverage is not detectable, that is equivalent to  $f = 1$ . Within the regions of emission lines the full covering of the AD flux yields only a part of the covering factor  $f = 0.7$  and the rest part of  $f$  is provided by the geometrical coverage factor  $g$  related solely to the BLR. As a result we assume that the flux coverage factor  $f$  is determined by a simple equation:

$$f = 0.7 + 0.3g. \quad (18)$$

<sup>2</sup> The fact that a continuum source can be fully associated with the AD is proved by observations of rapid continuum variability (see Peterson 1993 and references therein)

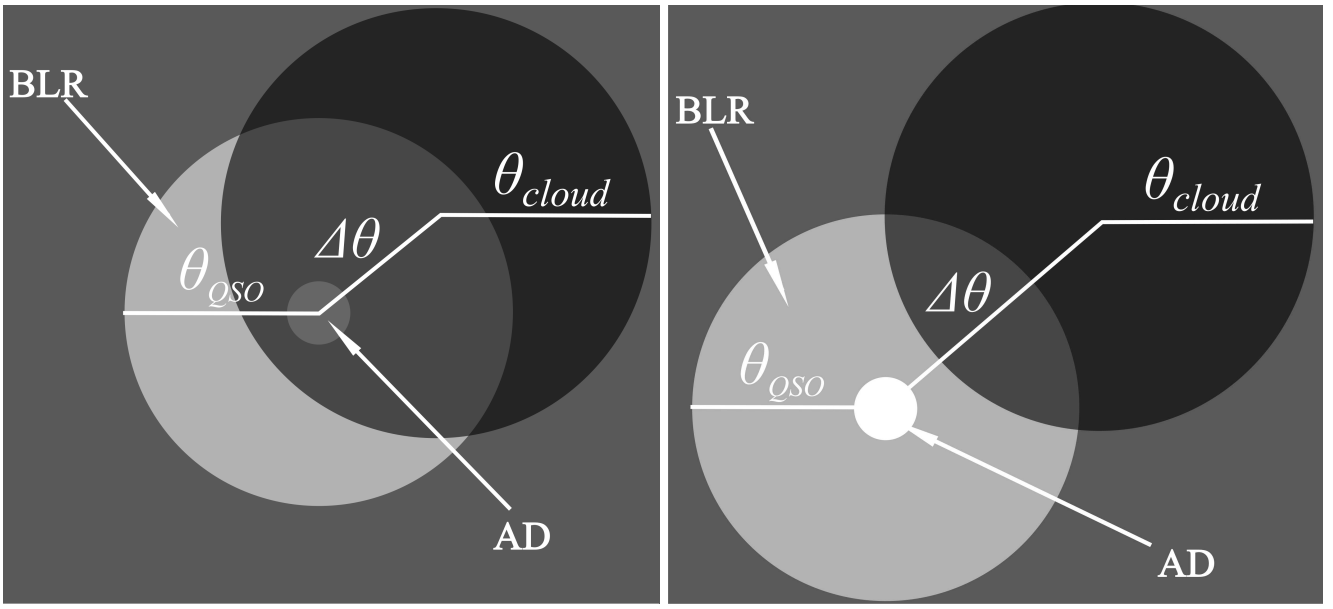


**Fig. 5** Model representation of radiation-flux nonuniformity. *Left panel:* the accretion disk of QSO is covered by a cloud totally,  $\Delta\theta < \theta_{cloud}$  ( $\delta < \rho$ ); *right panel:* the accretion disk of QSO is uncovered by a cloud,  $\Delta\theta > \theta_{cloud}$  ( $\delta > \rho$ ). The flux passing by the cloud contains the whole flux of the accretion disk and more than a half of flux emitted by the BLR. In both case the BLR is covered only partially, but the case represented on the right panel is unlikely to be detected (see Section 3.1 for details).

Then, the calculation of the CDF  $P(f < f_0)$  is reduced to calculation of  $P(g < (f_0 - 0.7)/0.3)$ , i.e. to pure geometrical approach. A scaling  $f_0 = 0.7 + 0.3g_0$  applied to the upper horizontal axis in the right panel of Fig. 4 allows one to transform the dependencies on  $g$  —  $P(g < g_0)$  into the dependencies on  $f$  —  $P(f < f_0)$ .

The most conservative estimation of the probability to find a partial coverage at the minimal level of the noncoverage factor  $1 - f_0 \geq 0.02$  or  $f_0 \leq 0.98$  (e.g. Klimenko et al. 2015) yields 11% (lower curve in the right panel of Fig. 4). Note, that to detect the residual flux at the bottom of lines (which typically include several pixels) at the level  $\sim 2\%$  it is necessary to obtain high resolution spectra with high signal to noise ratio,  $S/N \sim 30 - 50$ . Spectra registered with less  $S/N$  allow to detect only higher minimal level, e.g.  $1 - f_0 \gtrsim 0.1$  or  $f_0 \lesssim 0.9$ . It gives the lowest level of the probability:  $\sim 5\%$ . However, we suppose that the middle solid curve in Fig. 4 is more realistic. It gives the probability estimation of the order of 15% to reveal the partial coverage with  $f < 0.9$ . Thus, the effect of partial coverage of QSOs by intervening  $H_2$  ALSs characterized by noticeable probability to be revealed at the spectra analyses.

### 3.3 Dependencies of $f$ -distribution on redshifts

Let us consider dependencies of the probability distribution on the redshifts  $z_q$  and  $z_c$ . Taking into account

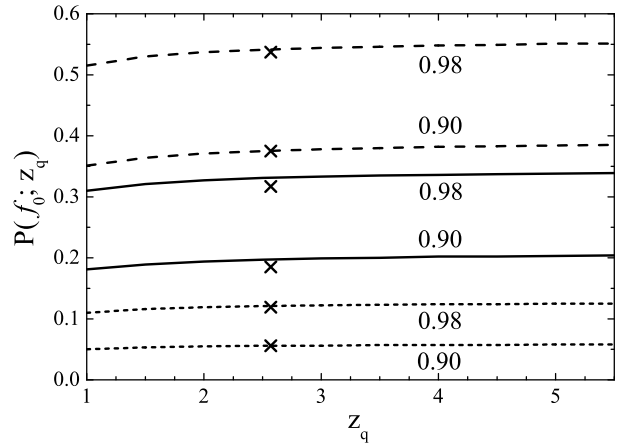


**Fig. 6** The cumulative distribution  $P(f_0; z_q) = P(f < f_0; z_q)$  (see text) as a function of QSO redshift,  $z_q$ , when a cloud redshift  $z_c = z_c(z_q)$  is maximally remote from  $z_q$  (see Eq. (20)). Types of lines are the same as in left panel of Fig. 4. Each pair of the curves corresponds to the same distribution of  $l_c$ ; the higher curve of a pair is plotted at  $f_0 = 0.98$ , while the lower one — at  $f_0 = 0.90$  (numbers near the curves). Crossed points correspond to the special case of  $P(f_0; z_q)$  calculated for Q1232+082 at  $z_q = 2.57$  and the  $H_2$ -cloud at  $z_c = 2.33$  registered in its spectrum.

dependence of the distribution  $p_\delta(\delta|\kappa)$  on  $z_q$  and  $z_c$ , defined by Eqs. (11) and (6), one can modify Eq. 10 and obtain CDF as

$$P(f < f_0; z_q, z_c) = \int_0^\infty \int_0^{\kappa[(f_0-0.7)/0.3, \delta, z_q, z_c]} p_\delta(\delta|\kappa, z_q, z_c) p_\kappa(\kappa) d\delta d\kappa, \quad (19)$$

where according to Eq. (18)  $f_0$  varies between 0.7 and 1.0, and the function  $\kappa$  is given in Eqs. (26) and (27).

Firstly, the dependence of the CDF on redshifts are expected to be small, since the angular diameter distance (see Eq. (5)) weakly depends on the redshifts within an interval  $z_c, z_q \sim 2 - 4$ . Let us consider an  $H_2$ -cloud, which is remote from the QSO by the maximal distance consistent with the very possibility to detect a set of  $H_2$  absorption lines in surrounding of a broad emission line and consequently to detect the partial coverage.

One can roughly formulate this condition of maximal removing as  $(1 + z_c) 1094 \text{ \AA} > (1 + z_q) 977 \text{ \AA}$ , where  $1094 \text{ \AA}$  is wavelength of L1-0 P(1) transition and  $977.02 \text{ \AA}$  corresponds to the C III prominent emission line in the restframe (see Fig. 7), since most of saturated  $H_2$  absorption lines are blueward in relation to  $1094 \text{ \AA}$  and all prominent emission lines of QSO spectra are redward in relation to  $977.02 \text{ \AA}$ . Note that we conservatively take L1-0 P(1) line as a boundary, since the most long-wavelength  $H_2$  transitions correspond to L0-0 band at  $\lambda \sim 1108 - 1110 \text{ \AA}$  (see Fig. 7) frequently appears as a unsaturated absorption lines and can not be used for confident detection of the partial coverage. Therefore, to obtain partial coverage of the QSO BLR by a  $H_2$ -cloud one needs that redshifts of  $H_2$  ALSs obey the condition

$$0.89 z_q - 0.11 \leq z_c \leq z_q, \quad (20)$$

where we put  $977/1094 \simeq 0.89$ . The right part of condition just indicates that  $H_2$  ALS is located between QSO and observer.

Fig. 6 demonstrates dependencies  $P(f_0; z_q) = P(f < f_0; z_q, z_c(z_q))$  on  $z_q$  at two fixed  $f_0 = 0.98$  and  $0.90$  and  $z_c(z_q)$  determined by minimal values of Eq. (20). One can see that the probability to reveal the flux coverage factor  $0.7 < f < f_0$  weakly depends on  $z_q$ . Moreover, the probability  $P(f_0, z_q, z_c)$  weakly depends also on  $z_c$ . Actually, it is demonstrated by crossed points in Fig. 6 calculated for the QSO 1232+082 ( $z_q = 2.57$ ) whose spectrum contains the  $H_2$  absorption system at  $z_c = 2.33$ . The crossed points lie closely to the corresponding curves  $P(f_0; z_q)$ , while the lower boundary  $z_c$  at  $z_q = 2.57$  according to Eq. (20) is  $z_c \geq 2.17$ , i.e. the

difference does not affect noticeably the value  $P(f_0; z_q)$ . Thus we can disregard approximately the dependence  $P(f_0; z_q)$  on  $z_c$ .

#### 4 Notes on observations of the partial coverage effect in QSO spectra

As an illustration Fig. 7 displays typical spectrum of the QSO in the restframe. Specifically we used the quasar spectrum J0003-2323 at  $z_q = 2.28$ . It was observed under program 166.A-0106 (PI: Jacqueline Bergeron). The data are in free access from the ESO database<sup>3</sup>. One can see strong  $Ly_\alpha$  emission line, a number of absorption lines of the Lyman-alpha forest imprinted in a continuum, damped Lyman-alpha absorption (DLA) system at  $\lambda_{DLA} = 1215 \text{ \AA} (1 + z_c)/(1 + z_q)$ , broad emission lines O IV,  $Ly_\beta$  and C III, and schematically a set of  $H_2$ -molecular absorption bands. We regard (see Section 3.1) that  $H_2$ -bearing clouds are supposed to be associated with DLA systems.

Fig. 8 shows the location of known  $H_2$  absorption systems at high redshifts on the  $z_q - z_c$  plane. All  $H_2$  systems capable to cause the partial coverage of QSO BLRs can be placed mainly between two linear bounds determined by Eq. (20). Fig. 8 represents also preliminary results of a systematic search of  $H_2$ -systems with traces of the partial coverage effect (Klimenko et al, in prep.). All five candidates marked by crosses in Fig. 8 have to be verified in further analysis.

#### 5 Conclusions

In this paper we estimate the probability of an incomplete coverage of the QSO BLR by the absorbing  $H_2$  molecular cloud. The key value of our analysis is a coverage factor  $f$  – a ratio of the flux of radiation which goes through a cloud to the total flux could have registered from the QSO without absorption by the cloud. We calculate the probability to obtain different coverage factors at given cosmological redshifts  $z_q$  and  $z_c$  of the QSO and cloud, respectively, employing the distribution of BLR sizes based on the data of the SDSS DR9, and a few model distributions of cloud sizes.

According to Fig. 4 the most conservative assessment of the probability to reveal the factor  $f < 0.98$  (observational minimum of noncoverage factor  $1 - f \geq 0.02$ ) is 11%. Thus one can expect at least three cases with  $f < 0.98$  from 27  $H_2$  absorption systems detected in QSO spectra up to now. The preliminary results of

<sup>3</sup><http://archive.eso.org>

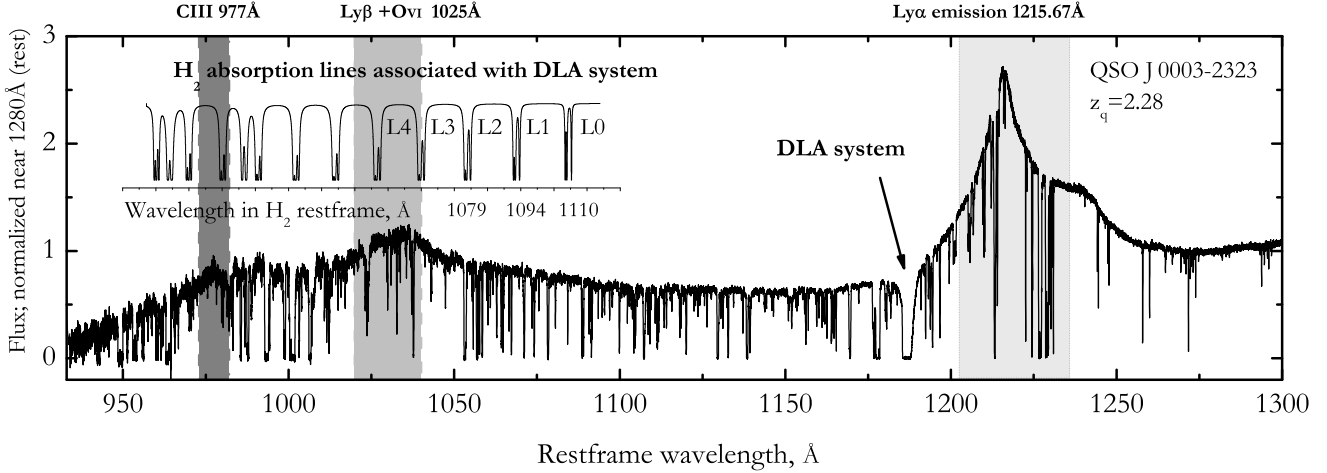


**Fig. 7** Spectrum of quasar J0003-2323 at  $z_q = 2.28$  shown in its own restframe. There are marked  $\text{Ly}\alpha$  emission line, DLA system at  $\lambda_{\text{DLA}} = 1215\text{\AA}(1+z_q)/(1+z_c)$ , broad emission lines OIV,  $\text{Ly}\beta$  and CIII, Grey vertical bands indicate the wavelength regions in surroundings of the broad emission lines where the effect of partial coverage could be mostly pronounced. In the upper left part of the figure it is shown also the series of typical absorption bands of the  $\text{H}_2$  molecules. The spectrum is not properly flux calibrated, since it was obtained using Ultra Violet Echelle Spectrograph at VLT. For data see the footnote in the Section 4.

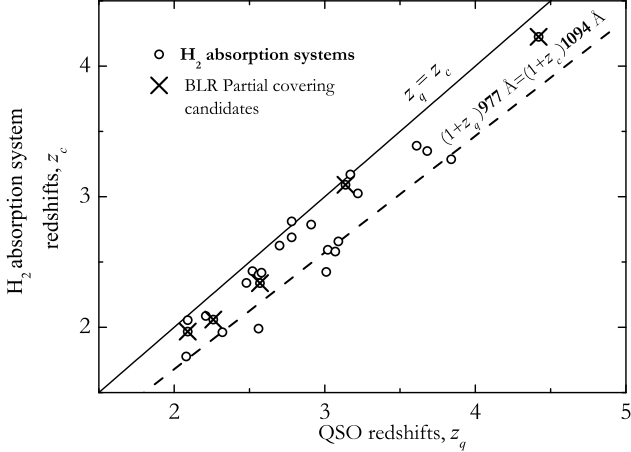


**Fig. 8** Known high-redshifted  $\text{H}_2$  absorption systems on the  $z_q - z_c$  plane. Empty circles indicate absorption systems, where partial coverage has not been detected up to now (22 objects); crosses mark systems for which a preliminary analysis evidences in favour of an occurrence of partially covered BLRs (5 objects) in QSOs spectra. The upper solid line corresponds to  $z_c = z_q$  and determines the highest positions of  $\text{H}_2$  systems on the  $z_q - z_c$  plane; the dashed line is  $z_c = 0.89z_q - 0.11$  (see Eq. (20)) and gives the lowest  $z_c$  at fixed  $z_q$  when partial coverage by intervening cloud can be detected. The data was taken from Ivanchik et al. (2015).

the systematic search of the partial coverage effect in quasar spectra with imprinted intervening  $\text{H}_2$  absorption systems give five cases, that is consistent with the prediction.

Systematic search for the partial coverage effect in the  $\text{H}_2$  absorption systems will allow to obtain restrictions on characteristic scales of the  $\text{H}_2$  clouds. For instance, relatively high frequency of revealing the effects of incomplete coverage with  $0.7 < f < 1.0$  would mean that cloud sizes are comparable with the BLR sizes, i.e.  $\sim 0.2 - 0.3$  pc. Relatively low frequency of such effects in QSO spectra would mean that the typical cloud size essentially exceeds the BLR size as it was widely accepted previously.

In this paper we consider a simple model, where absorption and emission regions are represented by spherical shape clouds. In case of asymmetrical and/or patchy structure of the absorption as well as emission regions the situation can be sufficiently complicated by increasing the number of parameters and uncertainties. However, it seems that estimate of the probability of revealing partial coverage – the main result of this paper, will not significantly changed. Our understanding of the structure, distribution of sizes and physical conditions of cold interstellar medium at high redshift would be constrained by the further observations and extension of the statistics of the BLRs partial coverage by  $\text{H}_2$  absorption clouds.

**Acknowledgements** This work is supported by the Russian Science Foundation, grant 14-12-00955.

## References

- Abdo, A.A., Ackermann, M., Ajello, M., Axelsson, M., Baldini, L., Ballet, J., Barbiellini, G., Bastieri, D., Baughman, B.M., Bechtol, K., et al.: *Nature* **463**, 919 (2010)
- Ahn, C.P., et al.: *Astrophys. J. Suppl. Ser.* **203**, 21 (2012)
- Balashev, S.A., Petitjean, P., Ivanchik, A.V., Ledoux, C., Srianand, R., Noterdaeme, P., Varshalovich, D.A.: *Mon. Not. R. Astron. Soc.* **418**, 357 (2011)
- Blackburne, J.A., Pooley, D., Rappaport, S., Schechter, P.L.: *Astrophys. J.* **729**, 34 (2011)
- Chelouche, D., Daniel, E.: *Astrophys. J.* **747**, 62 (2012)
- Ibata, R.A., Lewis, G.F., Irwin, M.J., Lehár, J., Totten, E.J.: *Astron. J.* **118**, 1922 (1999)
- Ivanchik, A.V., Petitjean, P., Balashev, S.A., Srianand, R., Varshalovich, D.A., Ledoux, C., Noterdaeme, P.: *Mon. Not. R. Astron. Soc.* **404**, 1583 (2010)
- Ivanchik, A.V., Balashev, S.A., Varshalovich, D.A., Klimenko, V.V.: *Astronomy Reports* **59**, 100 (2015)
- Jiménez-Vicente, J., Mediavilla, E., Muñoz, J.A., Kochanek, C.S.: *Astrophys. J.* **751**, 106 (2012)
- Kanekar, N., Lane, W.M., Momjian, E., Briggs, F.H., Chengalur, J.N.: *Mon. Not. R. Astron. Soc.* **394**, 61 (2009)
- Kaspi, S., Maoz, D., Netzer, H., Peterson, B.M., Vestergaard, M., Jannuzi, B.T.: *Astrophys. J.* **629**, 61 (2005)
- Kaspi, S., Brandt, W.N., Maoz, D., Netzer, H., Schneider, D.P., Shemmer, O.: *Astrophys. J.* **659**, 997 (2007)
- Kayser, R., Helbig, P., Schramm, T.: *Astron. Astrophys.* **318**, 680 (1997)
- Klimenko, V.V., Balashev, S.A., Ivanchik, A.V., Ledoux, C., Noterdaeme, P., Petitjean, P., Srianand, R., Varshalovich, D.A.: *Mon. Not. R. Astron. Soc.* **448**, 280 (2015)
- Kulkarni, G., Loeb, A.: *Mon. Not. R. Astron. Soc.* **422**, 1306 (2012)
- Ledoux, C., Theodore, B., Petitjean, P., Bremer, M.N., Lewis, G.F., Ibata, R.A., Irwin, M.J., Totten, E.J.: *Astron. Astrophys.* **339**, 77 (1998)
- Liszt, H.: *Astron. Astrophys.* **389**, 393 (2002)
- Noterdaeme, P., et al.: *Astron. Astrophys.* **547**, 1 (2012)
- Ofengeim, D.D., Ivanchik, A.V., Kaminker, A.D., Balashev, S.A.: *J. Phys.: Conf. Ser.* **461**(1), 012046 (2013)
- Peterson, B.M.: *Publ. Astron. Soc. Pac.* **105**, 247 (1993)
- Petitjean, P., Rauch, M., Carswell, R.F.: *Astron. Astrophys.* **291**, 29 (1994)
- Planck Collaboration, Ade, P.A.R., et al.: *Astron. Astrophys.* **571**, 16 (2014)
- Rauch, M.: *Annu. Rev. Astron. Astrophys.* **36**, 267 (1998)
- Sluse, D., Schmidt, R., Courbin, F., Hutsemékers, D., Meylan, G., Eigenbrod, A., Anguita, T., Agol, E., Wambsganss, J.: *Astron. Astrophys.* **528**, 100 (2011)
- Snow, T.P., McCall, B.J.: *Annu. Rev. Astron. Astrophys.* **44**, 367 (2006)
- Zeldovich, I.B., Novikov, I.D.: *Relativistic Astrophysics. Volume 2 - The Structure and Evolution of the Universe.* Chicago, Il, University of Chicago Press, (1983)

## Appendix

In Appendix we obtain an analytic approximations of  $g(\kappa, \delta)$  determined in Eqs. (9) and (8) and represented as a set of sections continuously sewed together in surroundings of definite boundary lines  $\kappa(\delta)$  (see below) at fixed  $z_c$  and  $z_q$ . Such an approach allows us to derive an appropriate set of simple reciprocal functions  $\kappa(g, \delta)$  and to use them in the integrations of Eqs. (10) and (19).

Firstly, using Eq. (6) one can define two basic boundary functions on  $\delta$  at the plane  $\delta - \kappa$ :

$$\kappa_1 = \frac{D(z_c)}{D(z_q)}|\delta - 1|, \quad \kappa_2 = \frac{D(z_c)}{D(z_q)}(\delta + 1). \quad (21)$$

These functions correspond to the boundaries  $\rho = |\delta - 1|$  and  $\rho = \delta + 1$ , respectively, at the plane  $\delta - \rho$ , which separate the *crescent-like coverage* region (iii) from the regions (ii), (iv) and (i) (see Fig. 2).

Then, to obtain simple approximations within the region (iii), we introduce two additional interfacing dependences on  $\delta$

$$\kappa_{1/3} = \frac{2}{3}\kappa_1 + \frac{1}{3}\kappa_2 \quad \kappa_{2/3} = \frac{1}{3}\kappa_1 + \frac{2}{3}\kappa_2, \quad (22)$$

and using Eqs. (8) and (6) calculate corresponding accurate functions

$$g_{1/3} = g(\kappa_{1/3}, \delta) \quad g_{2/3} = g(\kappa_{2/3}, \delta). \quad (23)$$

Note, that all defined quantities depend on  $z_q$  and  $z_c$ , which are incorporated in the dependences  $\kappa(\delta)$ .

To obtain the domain-like approximations for  $g(\kappa, \delta)$  it is convenient to introduce two basic zones: (a) with  $\delta \geq 1$  and (b) with  $\delta < 1$ .

In the zone (a) at  $\delta \geq 1$  we have:

$$g(\kappa, \delta) = \begin{cases} 0; & 0 < \kappa < \kappa_1 \\ g_{1/3} \left( \frac{\kappa - \kappa_1}{\kappa_{1/3} - \kappa_1} \right)^{3/2}; & \kappa_1 \leq \kappa < \kappa_{1/3} \\ g_{1/3} + (g_{2/3} - g_{1/3}) \frac{\kappa - \kappa_{1/3}}{\kappa_{2/3} - \kappa_{1/3}}; & \kappa_{1/3} \leq \kappa < \kappa_{2/3} \\ 1 - (1 - g_{2/3}) \left( \frac{\kappa_2 - \kappa}{\kappa_2 - \kappa_{2/3}} \right)^{3/2}; & \kappa_{2/3} \leq \kappa < \kappa_2 \\ 1; & \kappa_2 \leq \kappa, \end{cases} \quad (24)$$

where five sections consequently correspond (from top to bottom): 1-st section to the region (iv) at  $\rho < \delta - 1$ ;

2-nd, 3-d and 4-th sections to (iii) at  $\delta - 1 \leq \rho < \delta + 1$ ;  
5-th section to (i) at  $\delta + 1 \leq \rho$ .

In the zone (b) at  $\delta < 1$  we have:

$$g(\kappa, \delta) = \begin{cases} \rho^2(\kappa); & 0 < \kappa \leq \kappa_1 \\ \frac{g_{1/3} - \Delta}{\kappa_{1/3}^{3/2} - \kappa_1^{3/2}} \kappa^{3/2} + \frac{\kappa_{1/3}^{3/2} \Delta - \kappa_1^{3/2} g_{1/3}}{\kappa_{1/3}^{3/2} - \kappa_1^{3/2}}; & \kappa_1 \leq \kappa < \kappa_{1/3} \\ g_{1/3} + (g_{2/3} - g_{1/3}) \frac{\kappa - \kappa_{1/3}}{\kappa_{2/3} - \kappa_{1/3}}; & \kappa_{1/3} \leq \kappa < \kappa_{2/3} \\ 1 - (1 - g_{2/3}) \left( \frac{\kappa_2 - \kappa}{\kappa_2 - \kappa_{2/3}} \right)^{3/2}; & \kappa_{2/3} \leq \kappa < \kappa_2 \\ 1; & \kappa_2 \leq \kappa, \end{cases} \quad (25)$$

where  $\Delta = (1 - \delta)^2$ , five sections consequently correspond: 1-st upper section to the region (ii) at  $\rho < 1 - \delta$ ; 2-nd, 3-d and 4-th sections to (iii) at  $1 - \delta \leq \rho < 1 + \delta$ ; 5-th section to (i) at  $1 + \delta \leq \rho$ . Note that a difference between the exact coverage factor  $g(\kappa, \delta)$  and the approximations given by Eqs. (24) and (25) does not exceed 0.02.

Finally, we can obtain an approximation for the reciprocal function  $\kappa(g, \delta)$ , treating the same two zones: (a) with  $\delta \geq 1$  and (b) with  $\delta < 1$ .

Thus in the zone (a) at  $\delta \geq 1$  we have:

$$\kappa(g, \delta) = \begin{cases} \kappa_1 + (\kappa_{1/3} - \kappa_1) \left( \frac{g}{g_{1/3}} \right)^{2/3}; & 0 \leq g < g_{1/3} \\ \kappa_{1/3} + (\kappa_{2/3} - \kappa_{1/3}) \frac{g - g_{1/3}}{g_{2/3} - g_{1/3}}; & g_{1/3} \leq g < g_{2/3} \\ \kappa_2 - (\kappa_2 - \kappa_{2/3}) \left( \frac{1 - g}{1 - g_{2/3}} \right)^{2/3}; & g_{2/3} \leq g \leq 1, \end{cases} \quad (26)$$

where all three sections correspond to the region (iii) and its boundaries with the regions (iv) at  $g = 0$  and (i) at  $g = 1$ .

In the zone (b) at  $\delta < 1$  employing Eq. (6) we have:

$$\kappa(g, \delta) = \begin{cases} \frac{D(z_c)}{D(z_q)} \sqrt{g}; & 0 \leq g < \Delta \\ \left[ \frac{\kappa_{1/3}^{3/2} (g - \Delta) + \kappa_1^{3/2} (g_{1/3} - g)}{g_{1/3} - \Delta} \right]^{2/3}; & \Delta \leq g < g_{1/3} \\ \kappa_{1/3} + (\kappa_{2/3} - \kappa_{1/3}) \frac{g - g_{1/3}}{g_{2/3} - g_{1/3}}; & g_{1/3} \leq g < g_{2/3} \\ \kappa_2 - (\kappa_2 - \kappa_{2/3}) \left( \frac{1 - g}{1 - g_{2/3}} \right)^{2/3}; & g_{2/3} \leq g \leq 1, \end{cases} \quad (27)$$

where as in Eq. (25)  $\Delta = (1 - \delta)^2$ , and the first upper section corresponds to the region (ii), all three others to (iii).